Peer-reviewed version available at Membranes 2018, 8, 85; doi:10.3390/membranes8030085

Article

Dual Functional Ultrafiltration Membranes with Enzymatic Digestion and Thermo-Responsivity for Protein Self-Cleaning

Anbharasi Vanangamudi [1,2,*], Ludovic F. Dumée [2], Mikel Duke [1] and Xing Yang [1,*]

[1] Institute for Sustainable Industries & Liveable Cities, College of Engineering and Science, Victoria University, Melbourne, PO Box 14428, Victoria 8001, Australia; anbharasi.vanangamudi@live.vu.edu.au (A.V.); mikel.duke@vu.edu.au (M.D.); xing.yang@vu.edu.au (X.Y.)

[2] Deakin University, Waurn Ponds, Institute for Frontier Materials, Victoria 3216, Australia; ludovic.dumee@deakin.edu.au (L.D.)

* Correspondence: anbharasi.vanangamudi@live.vu.edu.au; Tel.: +61-399-197-640; xing.yang@vu.edu.au; Tel.: +61-399-197-690

Abstract: Controlling surface-protein interaction during wastewater treatment is the key motivation for developing functionally modified membranes. A new biocatalytic thermo-responsive poly(vinylidene fluoride)(PVDF)/nylon-6,6/poly(*N*-isopropylacrylamide)(PNIPAAm) ultrafiltration membrane was fabricated to achieve dual functionality of protein-digestion and thermo-responsive self-cleaning. The PVDF/nylon-6,6/PNIPAAm composite membranes were constructed by integrating a hydrophobic PVDF cast layer and hydrophilic nylon-6,6/PNIPAAm nanofiber layer where trypsin enzymes were covalently immobilized. The immobilization density of enzymes on the membrane surface decreased with increasing PNIPAAm concentration, due to the decreased number of amine functional sites. Through a ultrafiltration study using a model solution containing BSA/NaCl/$CaCl_2$, the PNIPAAm containing biocatalytic membranes demonstrated a combined effect of enzymatic and thermo-switchable self-cleaning. The membrane without PNIPAAm revealed superior fouling resistance and self-cleaning with an R_{PD} of 22%, compared to membranes with 2 and 4 wt% PNIPAAm with 26% and 33% R_{PD}, respectively, after an intermediate temperature cleaning at 50°C, indicating that higher enzyme density offers more efficient self-cleaning than the combined effect of enzyme and PNIPAAm at low concentration. The conformational volume phase transition of PNIPAAm did not affect the stability of immobilized trypsin on membrane surface. Such novel surface engineering design offer a promising route to severe surface-protein contamination remediation in food and wastewater applications.

Keywords: thermo-responsive; ultrafiltration; enzymes; self-cleaning; nanofibers

1. Introduction

Non-specific surface-protein interactions at the membrane interface during ultrafiltration (UF) leads to permanent fouling, by accumulation of protein contaminants on membrane surface or into pores [1]. Membrane fouling by proteins cause pore blockage and forms cake layer leading to rapid decline in membrane permeability, increase in cleaning frequency and diminished membrane performance [2,3]. One of the most versatile methods to reduce fouling and self-clean the membranes is to modify the membrane surface functionalities by incorporating self-cleaning materials such as hydrophilic copolymers [4,5], amphiphilic copolymers [6], zwitterionic compounds [7], metal oxides [8], biocatalytic enzymes [1,9], and responsive materials [5,10,11]. Self-cleaning materials are a class of materials with intrinsic ability to remove any contaminant from their surfaces via various mechanisms [12].

Biocatalytic enzymes are macromolecules that undergoes biochemical catalysis of specific substrates like proteins to produce respective products. Proteolytic enzymes have attracted attention as self-cleaning compounds that can lyse and detach the protein foulants from the membrane surface [1,13]. To overcome self-hydrolysis of free enzymes in solution leading to instability, deprived performance and poor reusability [14], enzymes may be immobilized onto suitable substrates. The nature and properties of the substrates play a significant role in enhancing enzyme loading, activity and stability over time and cleaning cycles [15].

Electrospun nanofibers are considered to be one of the most suitable substrates for enzyme immobilization due to their high surface-to-volume ratio which provides high enzyme loading and improved stability [16], as well as great structure versatility and facile control on surface chemistry [17,18]. The nanofiber membranes possess high porosity and pore interconnectivity that provides low hindrance to mass transfer making it suitable for filtration [19,20]. The activity of enzyme immobilized onto the nanofibers was found to be higher than that of enzyme immobilized commercially cast membranes, owing to the high surface area providing more active sites for enzyme immobilization [9,21,22]. Also, enzyme immobilized nanofibers presented good operational reusability. For example, trypsin immobilized onto polyethylene terephthalate (PET)/poly (lactic acid) (PLA) nanofiber mats and chitosan nanofibers presented 80% (eleven cycles) and 97% (five cycles) reusability respectively [23,24]. Nanofibers are typically used as a surface functional layer along with a support layer during the treatment of complex wastewater [25]. Despite showing enhanced membrane antifouling performance and enzyme resuability, the reported biocatalytic UF membranes exhibited low permeability [1,26,27]. Thus, biocatalytic antifouling membranes with stable enzyme attachment and engineered porous structure offering long term operational stability and high membrane permeability are desired. Since enzymes are susceptible to loss in activity over time [9,28], an additional self-cleaning material that provide facile membrane cleaning may be incorporated to achieve enhanced performance.

Thermo-responsive polymers are considered as one of the promising antifouling materials that offer facile temperature based cleaning for membranes [29]. Poly(N-isopropylacrylamide) (PNIPAAm) is a well-known temperature-sensitive polymer with a lower critical solution temperature (LCST) of about 32°C in an aqueous solution [30,31], below which the PNIPAAm polymer chains are more hydrophilic having an extended conformation in water. As the temperature is elevated above LCST, they become less hydrophilic forming a dehydrated compact structure exhibiting a sharp reversible volume-phase conformational transition providing strong inherent washing force. On one hand, the self-cleaning behaviour of the PNIPAAm containing membrane could be attributed to the enhanced hydrophilicity below its LCST, thus facilitating foulants desorption from the surface. For example, PNIPAAm grafted polydopamine/PET UF membranes recovered 90% of the initial flux at 20°C compared to unmodified PET membrane that showed only 76% flux recovery, ascribed to the enhanced surface hydrophilicity [29]. Similarly, a flux recovery of 92% was achieved for the poly (vinylidene fluoride) (PVDF)/TiO_2-g-PNIPAAm nanocomposite membranes compared to 47% flux recovery for the control PVDF membranes at 23°C [32]. On the other hand, the thermo-switchable characteristic of PNIPAAm providing strong inherent washing force was exploited to remove the membrane foulants in UF, exhibiting self-cleaning property. For example, the PNIPAAm grafted polyethylene membrane fouled by model protein bovine serum albumin (BSA) showed 97% flux recovery via applying a temperature-change (25°C/35°C) cleaning method [33]. Similarly, the PNIPAAm-grafted ZrO_2 membrane showed 80% flux recovery after temperature-change cleaning (25°C/35°C) of BSA fouled membranes [34]. However, the combined self-cleaning effect of PNIPAAm and biocatalytic enzymes has not been explored so far and the impact of one material on the other in terms of filtration and self-cleaning effect was not investigated. In this study, a new biocatalytic PVDF/nylon-6,6/PNIPAAm composite UF membrane was prepared by covalently immobilizing trypsin (TR) enzyme onto functional nanofibrous surface of PVDF/nylon-6,6/PNIPAAm membrane, to achieve dual functionality of protein-digestion and thermo-responsivity for self-cleaning effect. The structural and functional properties of the as-prepared membranes were investigated and correlated to the membrane performance in UF fouling experiments with

intermediate temperature cleaning. Also, the impact of thermo-switchable volume-phase transition on the stability of immobilized enzymes was studied. Figure 1 shows the schematic of membrane self-cleaning using enzymes and thermo-responsive PNIPAAm polymer via protein-digestion and volume phase transition mechanisms, respectively.

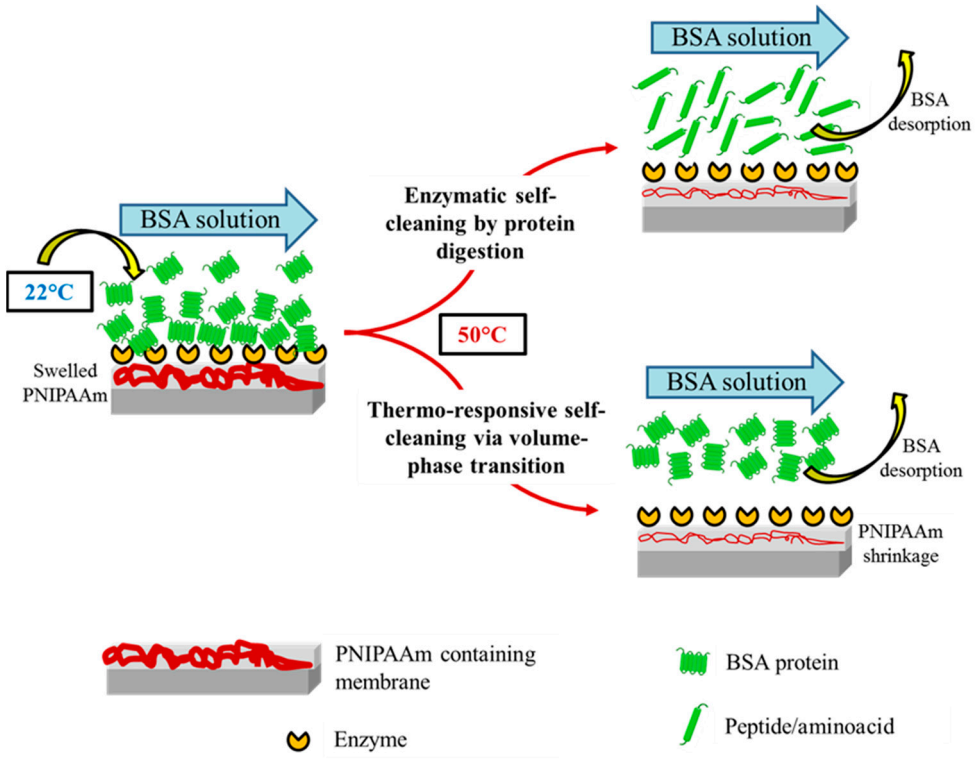

Figure 1. Conceptual schematic of self-cleaning biocatalytic and thermo-switchable membrane.

2. Experimental section

2.1. Materials

PVDF Kynar 761 grade (melting point 165-172°C) was purchased from Arkema Pte. Ltd., Singapore. Trypsin enzyme from porcine pancreas was purchased from Wako pure chemical industries Ltd (Osaka, Japan). The following chemicals were purchased from Sigma Aldrich (St. Louis, MO, USA) and used as received: PNIPAAm, (Mw 113 g/mol), polyamide-6,6 (nylon-6,6) (Mw 262.35 g/mol), poly(vinylpyrrolidone) (PVP-K-40) (Mw 40,000), 1-ethyl-3-(3-dimethylaminopropyl)carbodiimide (EDC), N-hydroxysuccinimide (NHS), BSA (Mw 66 kDa) as model protein, formic acid (>95%), analytical grade N,N'-dimethylacetamide (DMAC) (99.8%), trichloroacetic acid (TCA) (99%), ethanol (75%), glycerol (>99.5%), sodium chloride (NaCl) and calcium chloride (CaCl2). Deionized (DI) water used in all experiments was obtained from the Milli-Q plus system (Millipore, Bedford, MA, USA).

2.2. Preparation of PVDF/nylon-6,6/PNIPAAm membrane

The thermo-responsive PVDF/nylon-6,6/PNIPAAm composite membrane was prepared using a similar method used in our previous work [5]. Briefly, the composite membrane was prepared by three successive steps, (a) electrospinning a blend solution of 10 wt% nylon-6,6 and two different PNIPAAm concentrations (2 and 4 wt% PNIPAAm) in formic acid, at a voltage of 17 kV and flow rate of 0.25 mL/h with 150 mm tip to collector distance to construct thermo-responsive functional nanofiber mat, (b) conventional casting of the PVDF dope solution, which was prepared by continuous stirring of 18 wt% PVDF and 8 wt% PVP in DMAC solvent at 50°C overnight, on to the nanofiber mat and (c) phase inversion of the cast film on nanofiber mat by immersing into a

coagulation tank of DI water at 25°C to remove the solvent. The nascent membranes were post-treated by immersing in to a mixture of glycerol, ethanol and DI water in the ratio 2:1:2 (vol%) and was dried finally before characterisation. Similarly, the control PVDF/nylon-6,6 membrane was prepared without the addition of PNIPAAm.

2.3. Preparation of biocatalytic PVDF/nylon-6,6/PNIPAAm membranes

The immobilization of TR enzymes on to the as-prepared composite membranes with no PNIPAAm (PN0), 2 wt% (PN2) and 4 wt% (PN4) PNIPAAm were achieved by EDC/NHS coupling reaction using a similar method used in our previous study [9], to form PN0-TR, PN2-TR and PN4-TR membranes, respectively. Briefly, the enzyme carboxyl groups was first activated by reacting 1 mg/mL of enzyme solution with aqueous EDC and NHS in the ratio 4:1 for 1 h at room temperature, followed by the reaction of EDC/NHS activated enzymes with the primary amines on PN0-TR, PN2-TR and PN4-TR membranes for 12 h at 4°C to covalently attach on to the membranes via amide bonds. The membranes were then rinsed with DI water to remove the adsorbed TR. The efficiency of immobilization was calculated from the enzyme concentration decrease in solution before and after contact with the membrane.

2.4. Membrane characterization

The surface morphology of the biocatalytic composite membranes was observed using scanning electron microscopy (SEM) (ZEISS SUPRA 55VP, Germany) with an accelerating voltage of 5 kV and working distance of 10 mm. The membrane samples were sputter coated with a 5 nm layer of gold in high vacuum, using a Leica EM ACE600 prior to imaging using SEM. The average nanofiber diameters of the membranes were evaluated from the SEM images using ImageJ software. The pore size and pore size distribution of the membranes were measured using Porometer 3Gzh from Quantachrome. The Porofil™ wetted membrane samples of 25 mm diameter each were placed in the sample holder and was exposed to pressures from 6.4 to 34 bar for wet and dry run to measure the mean pore size. The pore size was measured three times for each membrane to obtain the average pore size. The dynamic water contact angles (CA_w) of the as-prepared membranes were measured using an optical contact angle meter CAM101 (KSV Instruments, Finland) to investigate the switchable surface hydrophilicity at 22°C (below LCST) and 50°C (above LCST). The required temperature of the membrane samples was achieved by adjusting the voltage of the source meter connected to the heating pad on which the samples are mounted. Prior optimisation of corresponding temperatures and feed voltages of the heating mats were established before mounting the heating pad on the contact angle meter. Rectangular strips of each membrane sample was pasted on to a glass slide by using sticky tape on the two corners of membrane, following which 4 µL water droplet was dispensed through a needle onto the membrane surface. Each measurement was recorded every 5 s over the duration of 60 s.

2.5. Quantification of immobilized TR and its activity against BSA

The surface density of immobilized TR on the as-prepared thermo-responsive composite membranes was calculated by measuring the enzyme concentration decrease in solution before and after contact with the membrane using UV-Visible spectrophotometer at 280 nm. Furthermore, the enzymatic activities of biocatalytic thermo-responsive membranes and free TR were determined by measuring their hydrolytic activities using the method described previously in our work with 1 wt% BSA solution as the substrate [9]. Briefly, the immobilized and free TR were allowed to react with the BSA solution for different time periods up to 1 h at 37°C and terminated by the addition of 5 wt% TCA. Then, the mixture was centrifuged at 2000xg and the absorbance of the supernatant containing hydrolytic products was measured at 280 nm using a UV-Visible spectrophotometer. The blank contained the supernatant of the reaction carried out as above using membranes without TR. One digestion unit (DU) represents an increase of 0.1 in absorbance of the hydrolytic products denoting an increase in the amount of substrate digested by the enzymes via hydrolysis.

2.6. Fouling studies

The antifouling and self-cleaning properties of the biocatalytic thermo-responsive membranes was evaluated using a cross flow UF set up having an effective area of 42×10^{-4} m^2 and flow velocity of 12.6 cm/s. The prepared feed solution contained 1 mg/mL BSA (model protein), 7 mM NaCl and 1 mM $CaCl_2$ in DI water that had a pH of 7.8 which falls within the optimal pH range of TR (pH 7.5-8.5) [35]. Each membrane was initially exposed to 10 min of compaction using DI water at 120 kPa at RT. It was then subjected to DI water containing 7 mM NaCl at 100 kPa for 15 min to measure the clean water permeance (P_w) in $L.m^{-2}.h^{-1}$ calculated by the following equation:

$$P_w = V/(A * t * p) \quad (1)$$

where V is the volume of permeate in L, A is the membrane area in m^2, t is the permeation time in h and p is the constant pressure (1 bar). Each UF experiment had 2 cycles and each cycle included the filtration of the prepared feed solution at 22°C for 1 h followed by an intermediate temperature cleaning with DI water at 22°C for 15 min. The number 'n' represented the cycle number. As a measure of protein fouling, the rate of permeance decline (R_{PD}) after each cycle was calculated using the equation,

$$RPD\ (\%) = \left[1 - \left(\frac{P_{e(n)}}{P_w}\right)\right] * 100 \quad (2)$$

where $P_{e(n)}$ is the final feed permeance in n^{th} cycle. Further, to study the self-cleaning property of membranes, the permeance recovery after the intermediate temperature cleaning at 22°C was calculated using the equation,

$$PRR\ (\%) = \frac{P_{w(n)}}{Pw} * 100 \quad (3)$$

where $P_{w(n)}$ is the clean water permeance in n^{th} cycle. Also, the fouling parameters namely reversible fouling (RF), irreversible fouling (IF) and total fouling (TF) for each cycle was computed by the following equations:

$$IF = [P_{w(n-1)} - P_{w(n)}]/P \quad (4)$$

$$RF = [P_{s(n)} - P_{e(n)}]/P \quad (5)$$

$$TF = IF + RF \quad (6)$$

where P_s is the initial feed permeance of each cycle and P_e is the final feed permeance of each cycle. Finally, SEM was used to visualise the surfaces of biocatalytic membranes after 2 cycles of filtration and compare the antifouling and self-cleaning properties of the enzyme immobilized membranes with and without PNIPAAm. Further, to investigate the combined antifouling and self-cleaning effects of protein-digestive enzymes and thermo-responsive PNIPAAm, 2 filtration cycles each including filtration of the prepared feed solution at 22°C for 1 h followed by an intermediate temperature cleaning with DI water at 50°C for 15 min were also performed and their respective R_{PD} was calculated for comparison.

2.7. Storage studies and effect of thermo-responsivity on enzyme stability

The biocatalytic membranes was stored under refrigeration at 4°C and at RT (22°C) and the enzyme activity was measured at regular intervals for up to two weeks. Further, the effect of thermo-switchable volume phase transition of the PNIPAAm on enzyme stability was investigated by measuring the hydrolytic activities of the as-prepared membranes (a) before and after treating the membranes at 50°C for 5 min and (b) over six consecutive reuse cycles before treating the membranes at 50°C for 5 min and after the treatment. These studies were conducted to investigate if the volume phase transition during thermo-switchable cleaning affects the stability of enzymes immobilized on

to the membrane surfaces. Treatment at 50°C for 5 min is exposing the membrane samples into DI water maintained at 50°C and mild stirring at 100 rpm for 5 min.

3. Results and Discussion

3.1. Enzyme distribution on membrane surface

The distribution of enzymes on the surface of PVDF/nylon-6,6/PNIPAAm and PVDF/nylon-6,6 membranes were analysed using the SEM imaging and shown in Figure 2. All the TR immobilized membranes with no PNIPAAm, 2 and 4 wt% PNIPAAm showed homogenous nanofiber structure with an average nanofiber diameter of 87±17 nm, 180±15 nm and 314±20 nm, respectively. The membrane with 4 wt% PNIPAAm show nano-branched structure with beads and clusters in some nanofibers that could be attributed to the uneven distribution of enzymes; while the membranes with no PNIPAAm and 2 wt% PNIPAAm showed homogenous enzyme attachment as seen in Figure 2. These clusters were formed due to possible aggregation of TR by randomized attachment points on the membrane implying the lack of control on enzyme immobilization [36]. Further, the thickness of the biocatalytic membranes with no PNIPAAm, 2 and 4 wt% PNIPAAm was measured from the cross sectional SEM micrographs to be 249±9 μm, 257±6 μm and 265±11 μm, respectively.

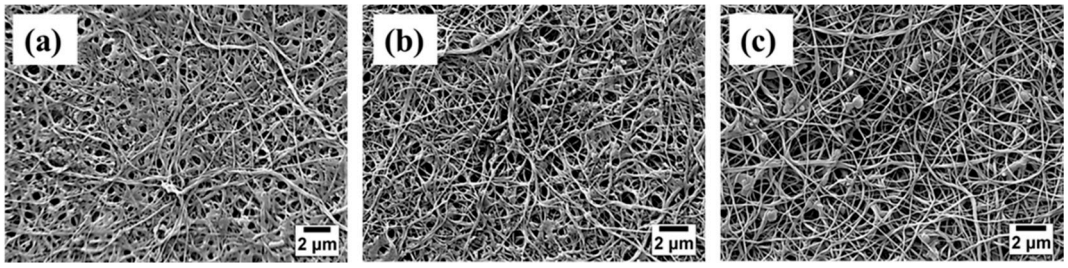

Figure 2. SEM images of biocatalytic membranes with (a) no PNIPAAm (PN0-TR); (b) 2 wt% PNIPAAm (PN2-TR); and (c) 4 wt% PNIPAAm (PN4-TR).

3.2. Surface density of immobilized enzyme

The density of immobilized TR on the surface of membranes was measured to study the amount of covalently attached enzymes and the results are presented in Figure 3. It was observed that the surface density of immobilized TR decreased as the PNIPAAm concentration in the membrane increased. This can be attributed to the incorporation of PNIPAAm in to the membrane which decreased the availability of surface amine functional groups from nylon-6,6 used for enzyme attachment via carbodiimide chemistry using EDC and NHS. The surface densities of immobilized TR on PVDF/nylon-6,6/PNIPAAm membranes with no PNIPAAm, 2 and 4 wt% PNIPAAm were 4.01 mg/m^2, 3.43 mg/m^2 and 2.87 mg/m^2, respectively, which were higher than the reported values of 0.7 mg/m^2 of TR immobilized PES membrane in the literature due to the nanofiber structure providing higher surface area for enhanced immobilization [1]. Among the prepared membranes, the control membrane without PNIPAAm had higher surface density of enzymes.

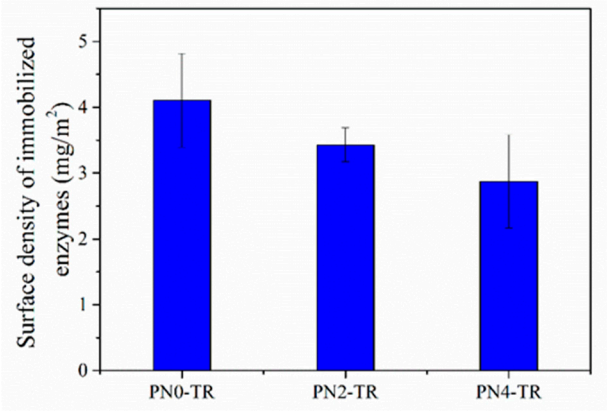

Figure 3. Surface densities of TR immobilized on to PVDF/nylon-6,6/PNIPAAm membranes with no PNIPAAm (PN0-TR), 2 wt% (PN2-TR) and 4 wt% (PN4-TR) PNIPAAm concentrations.

3.3. Membrane characterization

To evaluate the hydrophilicity and responsivity of biocatalytic thermo-responsive membranes, the dynamic water contact angles (CA_w) were measured over 60 s at 22°C and 50°C and are given in Figure 4a and 4b, respectively. The CA_w for the PNIPAAm containing membranes at 22°C exhibit a slightly faster attenuation compared to control membrane, as shown in Figure 4a. This decreasing tendency could be due to the addition of PNIPAAm that has a hydrophilic extended conformation below its LCST (32°C) which absorbs water by forming hydrogen bond between the amide groups of PNIPAAm and water, in spite of having lesser immobilized enzymes compared to control membrane. Also, at 22°C, the biocatalytic PVDF/nylon-6,6/PNIPAAm membrane with 2 wt% PNIPAAm showed the lowest CA_w of 13.6° compared to the membrane with 4 wt% PNIPAAm (18.4°) after 60 s, which may be ascribed to the increased amount of immobilized TR on the membrane surface. Figure 4b shows the dynamic CA_w of the as-prepared membranes at 50°C. For the PVDF/nylon-6,6 without PNIPAAm, the CA_w attenuation was similar at both 22°C and 50°C. However, the initial CA_w values for PNIPAAm containing membranes were higher at 50°C compared to those at 22°C, owing to the hydrophobic nature of the membrane above LCST that breaks the hydrogen bonds between amide groups of PNIPAAm and water molecules.

To investigate the volume-phase transition of the PNIPAAm around its LCST, the thermo-switchable CA_w of the membranes was measured and compared in terms of their initial CA_w at 22°C and 50°C, as shown in Figure 4a and 4b, respectively. The biocatalytic membrane without PNIPAAm exhibited no CA_w switchability; while the membranes with 2 and 4 wt% PNIPAAm exhibited switchable CA_w from 43.5° to 59° and from 44.8° to 61.8°, respectively, between 22°C and 50°C. The slightly higher switchability of biocatalytic membrane with 4 wt% PNIPAAm compared to membrane with 2 wt% PNIPAAm is attributed to increased PNIPAAm concentration in the membrane. However, this CA_w variation is more significant than the PVDF-g-PNIPAAm membrane reported in literature that exhibited switching CA_w from 87.5° (22°C) to 89° (50°C) [37].

The mean pore size and overall pore size distributions of the as-prepared membranes were measured using a capillary-flow porometer [5]. Figure 4c compares the differential pore distributions of the three membranes in terms of pore diameters. The TR immobilized PVDF/nylon-6,6 membrane exhibited narrow distribution curve due to the homogenously attached enzymes; while the TR immobilized membranes with 2 and 4 wt% PNIPAAm exhibited bimodal distribution curves owing to the formation of non-homogenous pore structures due to TR immobilization. The TR immobilized membrane with 4 wt% PNIPAAm membrane showed slightly wider distribution, possibly due to the clustering of TR enzymes as observed in Figure 2. The mean pore size of the TR immobilized PVDF/nylon-6,6/PNIPAAm membranes with no PNIPAAm, 2 and 4 wt% PNIPAAm were 44, 33 and 23 nm, respectively. The smaller pore size of the as-prepared membrane with 4 wt% PNIPAAm compared to those membranes with no PNIPAAm and 2 wt% PNIPAAm is ascribed to the formation of enzyme clusters on the membrane surface (Figure 2c).

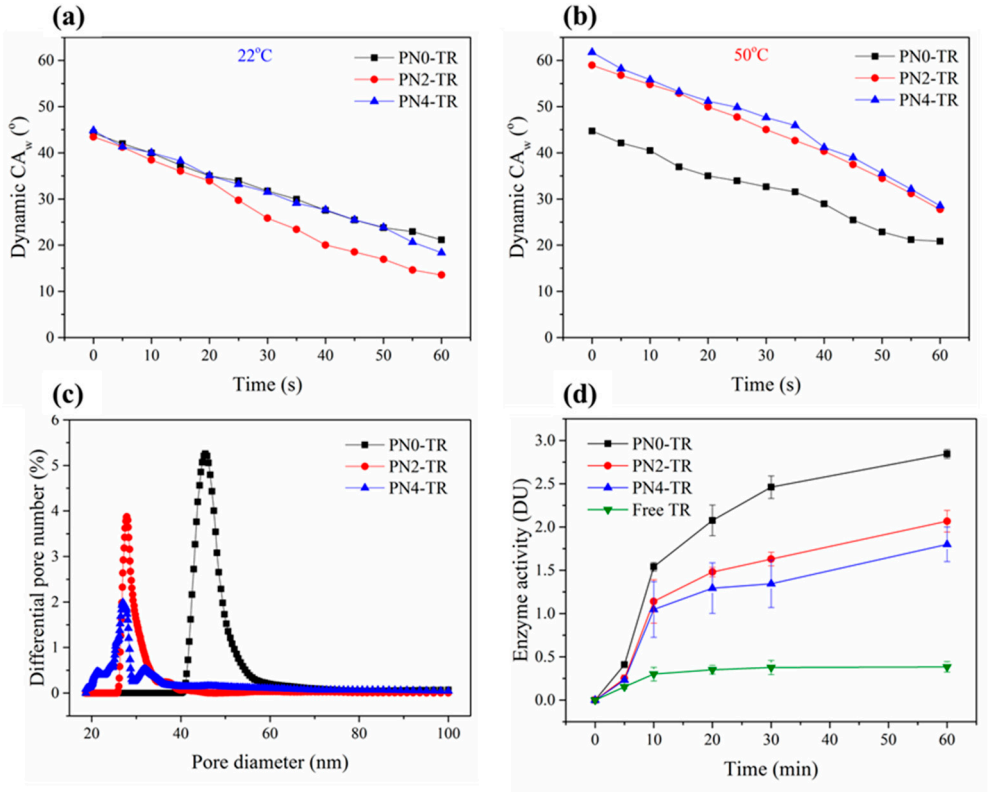

Figure 4. Dynamic water contact angles (CAw) of the biocatalytic membranes with and without PNIPAAm for 60 s contact time at (a) 22°C and (b) 50°C; (c) differential pore number (in %) distributions and (d) enzymatic activities of biocatalytic membranes over time with no PNIPAAm, 2 and 4 wt% PNIPAAm.

3.4. Enzyme activity evaluation across the nano-composite membranes

The enzymatic activity of the free and immobilized TR were determined by performing the hydrolytic assay using 1 wt% BSA solution which gives the amount of hydrolytic products formed. One digestion unit (DU) represents an increase of 0.1 in absorbance of the hydrolytic products denoting an increase in the amount of substrate digested by the enzymes. The results are shown in Figure 4d with respect to the reaction time. The amount of products formed by immobilized TR were noticed to be much greater than that of the free enzymes for all reaction times up to 60 min. For instance, at 60 min, the TR immobilized on to the membranes with no PNIPAAm, 2 and 4 wt% PNIPAAm produced about 7.5, 5.5 and 4.7 times more peptide products, respectively, than the free TR. It was also observed that the activity of immobilized TR increased with reaction time, whereas for the free enzymes, the activity increased initially but reached plateau in 10 min. This is due to the autolytic behaviour of the native enzymes, commonly known as self-digestion [38-40], while the increased stability of immobilized TR has greatly enhanced the enzymatic activity. The results further revealed that the PVDF/nylon-6,6 membrane without PNIPAAm show superior enzyme activity than the PNIPAAm containing membranes, possibly due to high immobilization density (Figure 3).

3.5. Protein fouling studies

The combined enzymatic and thermo-responsive effect on surface-protein interaction of the as-prepared biocatalytic membranes was investigated by conducting the filtration experiments with and without temperature-change cleaning, i.e., two-cycle filtration with respective intermediate DI water cleaning at 22°C and 50°C, with results shown in Figure 5 and 7, respectively.

Figure 5 shows the results of two consecutive filtration cycles with intermediate DI water cleaning at 22°C presented in terms of permeance and R_{PD} as a measure of protein fouling, and PRR, RF, TF and IF, as measures of the self-cleaning ability of the membranes. As presented in Figure 5a,

the biocatalytic membranes with 2 wt% (506 $L.m^{-2}.h^{-1}.bar^{-1}$) and 4 wt% (442 $L.m^{-2}.h^{-1}.bar^{-1}$) PNIPAAm exhibited slightly lower initial water permeance i.e. 13% and 24% lesser, compared to the membrane without PNIPAAm (581 $L.m^{-2}.h^{-1}.bar^{-1}$), which is attributed to the decrease in pore size due to the incorporation of PNIPAAm (Figure 4). Based on the permeance patterns observed for all membranes in Figure 5a, the R_{PD} was calculated based on Equation 2 and presented in Figure 5b to indicate the resistance to protein fouling. During the first filtration cycle, the biocatalytic PVDF/nylon-6,6/PNIPAAm membranes with no PNIPAAm, 2 and 4 wt% PNIPAAm suffered fouling as indicated by an R_{PD} of about 19%, 33% and 39%, respectively. The lower R_{PD} of biocatalytic membrane without PNIPAAm suggests that the membrane with higher density of immobilized enzymes with increased proteolytic ability i.e., protein digestive feature, were able resist BSA fouling to a larger extent [38]. Also, this result was found to be promising compared to the reported TR immobilized PMAA-g-PES UF membrane having a flux decline rate of 19.1% using a pure BSA solution of 1 g/L [1].

Further, during the second filtration cycle, the R_{PD} values were 22%, 39% and 45% for respective biocatalytic membranes with no PNIPAAm, 2 and 4 wt% PNIPAAm, after temperature cleaning at 22°C. Similar to first filtration cycle, the increasing R_{PD} follows the decreasing trend of immobilized TR density on the membrane surface. The SEM micrographs of the fouled membranes are presented in Figure 6. Consistent to the permeance results, the biocatalytic PVDF/nylon-6,6/PNIPAAm membrane with 4 wt% PNIPAAm showed heavy fouling (Figure 6c) compared to that without PNIPAAm that exhibited much reduced protein deposition presenting clear surface after two filtration cycles (Figure 6a), followed by the membrane with 2 wt% PNIPAAm that showed regional accumulation of protein (Figure 6b).

The self-cleaning ability of the biocatalytic membranes without temperature cleaning was quantified by calculating the PRR and fouling parameters namely RF, IF and TF. Figure 5c reveals that after the first filtration cycle, the biocatalytic membranes with no PNIPAAm, 2 and 4 wt% PNIPAAm were able to recover about 90%, 89% and 82% of the initial permeance, respectively. The greater permeance recovery of membranes with no PNIPAAm and 2 wt% PNIPAAm compared to that with 4 wt% PNIPAAm was attributed to the higher density of immobilized enzymes on the membrane surface that leads to breakdown of proteins into smaller polypeptides releasing them subsequently from the membrane surface. This result was found to be comparable with the literature work where TR immobilized PVDF MF membrane fabricated via a complex electron beam method showed 90% flux recovery after first filtration cycle with pure BSA solution of 3 g/L after backwashing with 120 mL of pure water every 1.6 L of filtration and self-cleaning through trypsin activation by immersing the fouled membrane into a buffered solution at 37 °C and pH 8.0 overnight [27]. Similar trend was observed after the second filtration cycle with biocatalytic membranes with no PNIPAAm, 2 and 4 wt% PNIPAAm showing 85%, 78% and 76% permeance recovery, respectively. The corresponding IF and RF parameters are presented in Figure 5d. After the first filtration cycle, the membranes with no PNIPAAm and 2 wt% PNIPAAm reduced the IF by 43% and 41%, respectively, compared to that with 4 wt% PNIPAAm, explaining the higher PRR presented in Figure 5c. This result demonstrates that less permanent fouling occurs with more enzymes featuring the self-cleaning capacity of the biocatalytic membranes. Thus, the membranes with higher density of immobilized enzymes exhibited much lower TF, which is corresponding to their higher PRR. Here, the biocatalytic PVDF/nylon-6,6 membrane without PNIPAAm was identified to be the best performing biocatalytic membrane in terms of fouling mitigation and self-cleaning ability.

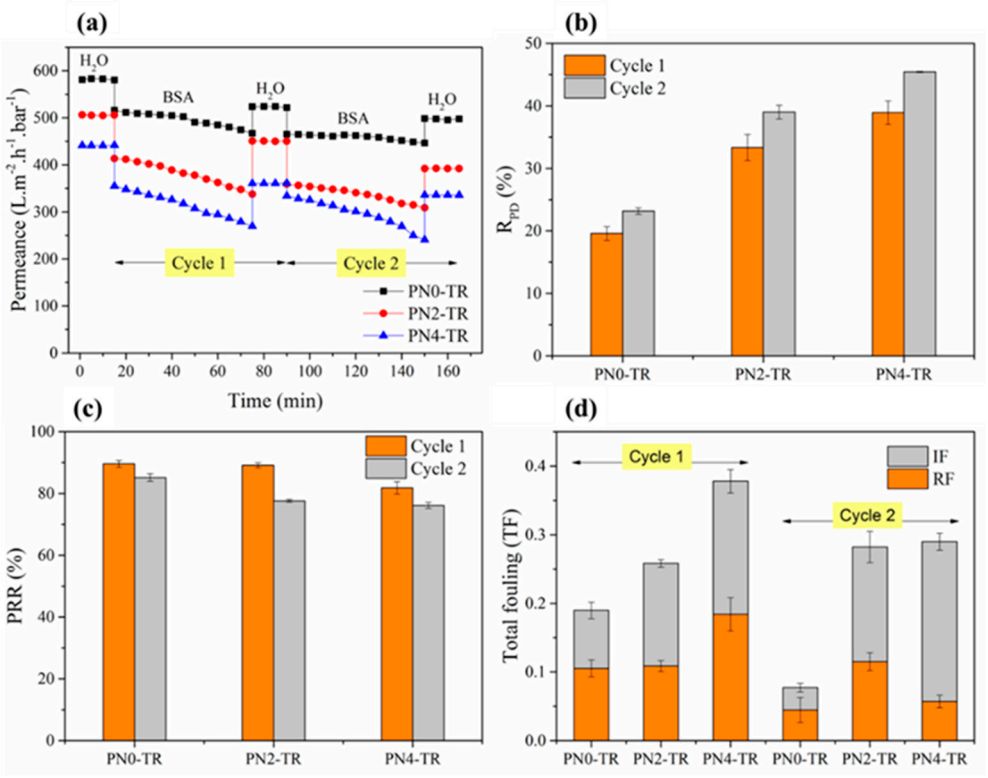

Figure 5. Protein fouling studies for biocatalytic membranes with and without PNIPAAm. (a) Permeance values for two filtration cycles. (b) RPD after each filtration cycle. (c) PRR after each filtration cycle. (d) TF, IF and RF for 2 filtration cycles. Experimental Conditions: Pressure = 100 kPa, cross-flow velocity = 12.6 cm/s, feed solution = 1 g/L BSA, 1 mM $CaCl_2$, 7 mM NaCl, both filtration and cleaning temperature = 22°C.

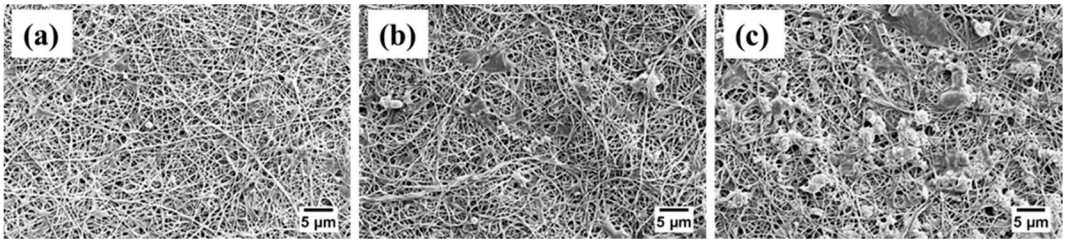

Figure 6. SEM micrographs of BSA fouled biocatalytic membranes with (a) no PNIPAAm (PN0-TR); (b) 2 wt% (PN2-TR); and (c) 4 wt% (PN4-TR) PNIPAAm after two filtration and cleaning cycles at 22°C.

To investigate the effect of PNIPAAm in the membrane matrix, the as-prepared biocatalytic PNIPAAm membranes were evaluated with the same filtration experiments, but involved temperature-change cleaning with DI water at 50°C. The performance results in terms of permeance and R_{PD} for two filtration cycles are given in Figure 7a and 7b, respectively. As shown in Figure 7a, the biocatalytic membranes with no PNIPAAm (556 $L.m^{-2}.h^{-1}.bar^{-1}$), 2 wt% (491 $L.m^{-2}.h^{-1}.bar^{-1}$) and 4 wt% (422 $L.m^{-2}.h^{-1}.bar^{-1}$) exhibited similar initial water permeance to those presented in Figure 5a, showing good repeatability. During the first filtration cycle, the R_{PD} values for biocatalytic PVDF/nylon-6,6/PNIPAAm membranes with no PNIPAAm, 2 and 4 wt% PNIPAAm were 18%, 22% and 30%. Further, during the second filtration cycle, the R_{PD} values were 22%, 26% and 33% for the respective membranes. The increasing trends of the R_{PD} in both cycles are consistent with those in Figure 3 corresponding to increasing density of enzymes on the membrane surface. Nevertheless, these values were found to be lower than the R_{PD} values reported with intermediate cleaning at 22°C in Figure 5b. Also, from Figure 7a, during the second filtration cycle, the membranes with no PNIPAAm, 2 wt% and 4 wt% PNIPAAm recovered about 91%, 93% and 96% of the initial BSA

permeance of first filtration cycle. Thus, in addition to the enzymatic protein digestive feature of the membrane, the temperature-change cleaning has confirmed the role of PNIPAAm on the antifouling and self-cleaning effects via thermo-switchable cleaning when the environment temperature switches from 22°C to 50°C. Overall, the as-prepared biocatalytic membrane without PNIPAAm revealed superior fouling resistance with reduced protein interactions compared to PNIPAAm containing membranes, indicating that higher degree of enzyme immobilization offers better self-cleaning than the combined effect at low enzyme and PNIPAAm concentrations. However, enzymes may suffer from deteriorating performance due to loss in biocatalytic activity over time [9,28] and hence further optimization of PNIPAAm concentration could be performed to achieve maximum thermo-switchable feature that further enhances the self-cleaning efficiency of membranes.

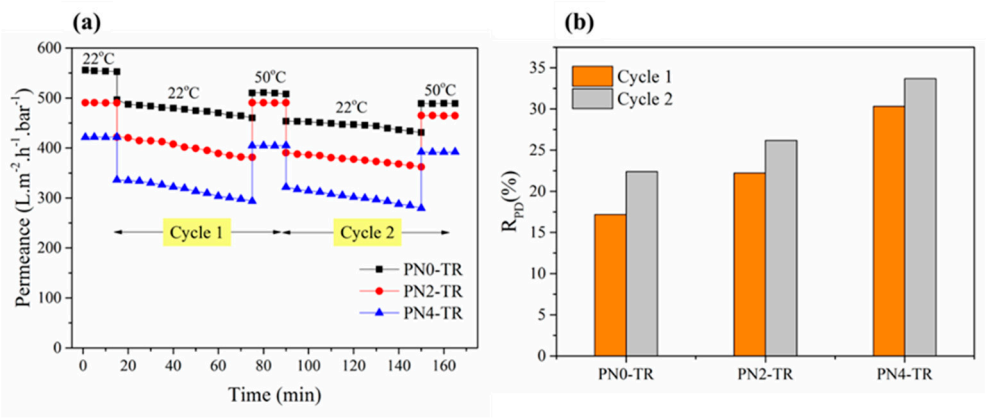

Figure 7. Protein fouling studies for biocatalytic membranes with and without PNIPAAm. (a) Permeance values for two filtration cycles. (b) RPD after each filtration cycle. Experimental Conditions: Pressure = 100 kPa, cross-flow velocity = 12.6 cm/s, feed solution = 1 g/L BSA, 1 mM $CaCl_2$, 7 mM NaCl, filtration temperature = 22°C, cleaning temperature = 50°C.

3.6. Storage studies & effect of thermo-responsivity on enzyme stability

The effect of storage time on the hydrolytic activities of the immobilized TR at 4°C and RT (22°C) were analysed and given in Figure 8a and 8b, respectively. It was revealed that at both RT and 4°C, the biocatalytic membrane without PNIPAAm retained about 81% and 78% of their initial enzymatic activities after 7 days, respectively, and about 71% and 69% of their initial activities after 14 days of storage. The activity results were found to be similar to the TR immobilized PVDF/nylon-6,6/chitosan membrane that was prepared in our earlier study [9] with 81% (RT) and 70% (4°C) detainment of initial enzyme activity after 7 and 14 days of storage, respectively, showing good reproducibility. Thus, the prepared membranes may not require inconvenient refrigerated storage conditions and can be stored at RT. Similarly, the membranes with 2 and 4 wt% PNIPAAm stored at RT retained about 79% and 76% of the activity after 7 days, respectively, and about 69% and 64% of the initial activity after 14 days, respectively.

The effect of thermo-switchable volume phase transition of the as-prepared membranes on the activities of freshly immobilized and used TR enzymes was investigated and the respective results are given in Figure 8c and 8d. In Figure 8c, the enzyme activities of biocatalytic membranes with no PNIPAAm, 2 and 4 wt% PNIPAAm declined only about 9%, 11% and 12% after treating at 50°C, which is similar to the storage data (Figure 8a and 8b) that did not affect the immobilized enzymes of PNIPAAm membranes. The enzyme activity of membrane with 4 wt% PNIPAAm declined most significantly by 12%, which is more than that without PNIPAAm (9%), possibly owing to the leaching of weakly attached TR enzyme clusters formed through aggregation on the membrane surface as observed in Figure 2. Similarly, in Figure 8d, the enzyme activities of as-prepared membranes after six consecutive reuse cycles and treatment at 50°C dropped less than about 3% after treating at 50°C. This could be due to the stable enzyme activity at both 22°C and 50°C temperatures and during conformational volume phase transition when the temperature switches from 22°C to 50°C. Further, from Figure 8d, the hydrolytic activities of immobilized enzymes declined with increasing reuse

cycles (up to six cycles), that may have occurred due to (a) the release of weakly bound enzymes, if any, and (b) the gradual change of fibrous morphology because of swelling and disintegration due to high hydrophilicity [28]. Also, the biocatalytic membranes with 2 and 4 wt% PNIPAAm show faster decline compared to the PNIPAAm-free membrane which may also be due to the loss of enzyme activity via change in nanofiber morphology via swelling and disintegration. Thus, the thermo-switchable volume phase transition of the as-prepared membranes was not found to affect the enzyme activity that was stable when temperature switched from 22°C to 50°C.

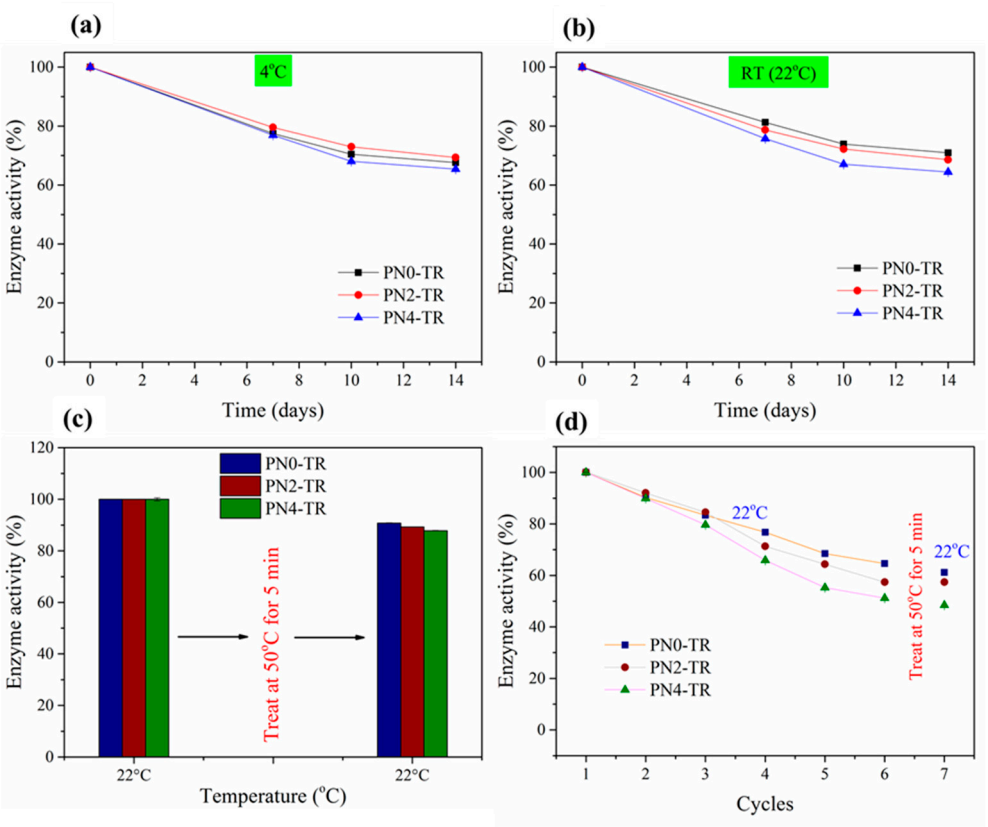

Figure 8. Hydrolytic activities of biocatalytic membranes for up to 14 days of storage at (a) 4°C and (b) 22°C; Stability of enzymes immobilized on to membranes in terms of enzyme activity with 50°C treatment for 5 min after (a) one reuse cycle and (b) six reuse cycles.

4. Conclusions

Biocatalytic membranes with and without PNIPAAm were successfully fabricated by immobilizing trypsin enzymes onto hydrophilic nylon-6,6/PNIPAAm nanofibrous layer supported by hydrophobic PVDF cast layer. It was demonstrated that superior enzyme loading on to the membrane without PNIPAAm can be achieved compared to PNIPAAm containing membranes, owing to the amine-rich and high surface to volume ratio of the nanofibrous structure. The trypsin immobilized membranes minimized surface-protein interaction on the surface, induced by enzyme proteolytic digestion. Through a dedicated UF study using model feed solution containing BSA, $CaCl_2$ and NaCl, the biocatalytic membrane without PNIPAAm offered superior performance in separation and purification applications, where they are more permeable and less fouled than the other membranes with PNIPAAm, demonstrating that higher degree of enzyme immobilization offers better self-cleaning than the combined self-cleaning of low concentrations of enzyme and PNIPAAm. Also, the thermo-switchable conformational volume phase transition of the as-prepared membranes did not affect the stability of surface immobilized enzymes. Hence, the approach of enzyme immobilization onto nanofibrous surface has greater potential including fouling mitigation and surface self-cleaning beyond membrane separation.

Author Contributions: The experimental work was designed and carried out by Ms. Anbharasi Vanangamudi under the guidance of Dr. Ludovic Dumee, Prof. Mikel Duke and Dr. Xing Yang. The manuscript was written by Ms. Anbharasi Vanangamudi and reviewed by all authors. All authors have given approval to the final version of the manuscript.

Funding: This research received no external funding

Acknowledgments: This work was supported by Victoria India Institute via Victoria India Doctoral Scholarship. Dr. L. DUMEE acknowledges the Australian Research Council (ARC) for his DECRA fellowship (DE180100130). Dr Xing Yang would like to acknowledge Victoria University for the Industry Postdoctoral Fellowship. The Microscopy platform at Deakin University and support from the technical team is also acknowledged.

Conflicts of Interest: The authors declare no conflict of interest.

References

1. Shi, Q.; Su, Y.; Ning, X.; Chen, W.; Peng, J.; Jiang, Z. Trypsin-enabled construction of anti-fouling and self-cleaning polyethersulfone membrane. *Bioresource Technology* **2011**, *102*, 647-651.
2. Jim, K.J.; Fane, A.G.; Fell, C.J.D.; Joy, D.C.]fouling mechanisms of membranes during protein ultrafiltration. *Journal of Membrane Science* **1992**, *68*, 79-91.
3. Ho, C.-C.; Zydney, A.L. A combined pore blockage and cake filtration model for protein fouling during microfiltration. *Journal of Colloid and Interface Science* **2000**, *232*, 389-399.
4. Zhao, Z.; Zheng, J.; Wang, M.; Zhang, H.; Han, C.C. High performance ultrafiltration membrane based on modified chitosan coating and electrospun nanofibrous pvdf scaffolds. *Journal of Membrane Science* **2012**, *394–395*, 209-217.
5. Vanangamudi, A.; Dumée, L.F.; Duke, M.C.; Yang, X. Nanofiber composite membrane with intrinsic janus surface for reversed-protein-fouling ultrafiltration. *ACS Applied Materials & Interfaces* **2017**, *9*, 18328-18337.
6. Zhu, L.-P.; Yi, Z.; Liu, F.; Wei, X.-Z.; Zhu, B.-K.; Xu, Y.-Y. Amphiphilic graft copolymers based on ultrahigh molecular weight poly(styrene-alt-maleic anhydride) with poly(ethylene glycol) side chains for surface modification of polyethersulfone membranes. *European Polymer Journal* **2008**, *44*, 1907-1914.
7. Zhao, X.; He, C. Efficient preparation of super antifouling pvdf ultrafiltration membrane with one step fabricated zwitterionic surface. *ACS Applied Materials & Interfaces* **2015**, *7*, 17947-17953.
8. Prince, J.A.; Bhuvana, S.; Anbharasi, V.; Ayyanar, N.; Boodhoo, K.V.K.; Singh, G. Self-cleaning metal organic framework (mof) based ultra filtration membranes - a solution to bio-fouling in membrane separation processes. *Sci. Rep.* **2014**, *4*.
9. Vanangamudi, A.; Saeki, D.; Dumée, L.F.; Duke, M.; Vasiljevic, T.; Matsuyama, H.; Yang, X. Surface-engineered biocatalytic composite membranes for reduced protein fouling and self-cleaning. *ACS Applied Materials & Interfaces* **2018**.
10. Chede, S.; Escobar, I.C. Fouling control using temperature responsive n-isopropylacrylamide (nipaam) membranes. *Environmental Progress & Sustainable Energy* **2016**, *35*, 416-427.
11. Rana, D.; Matsuura, T. Surface modifications for antifouling membranes. *Chemical Reviews* **2010**, *110*, 2448-2471.
12. Velicangil, O.; Howell, J.A. Self-cleaning membranes for ultrafiltration. *Biotechnology and Bioengineering* **1981**, *23*, 843-854.

13. Cordeiro, A.L.; Werner, C. Enzymes for antifouling strategies. *Journal of Adhesion Science and Technology* **2011**, *25*, 2317-2344.
14. Sun, L.; Liang, H.; Yuan, Q.; Wang, T.; Zhang, H. Study on a carboxyl-activated carrier and its properties for papain immobilization. *Journal of Chemical Technology & Biotechnology* **2012**, *87*, 1083-1088.
15. Ansari, S.A.; Husain, Q. Potential applications of enzymes immobilized on/in nano materials: A review. *Biotechnology Advances* **2012**, *30*, 512-523.
16. Kim, J.; Grate, J.W.; Wang, P. Nanostructures for enzyme stabilization. *Chemical Engineering Science* **2006**, *61*, 1017-1026.
17. Wang, Z.-G.; Wan, L.-S.; Liu, Z.-M.; Huang, X.-J.; Xu, Z.-K. Enzyme immobilization on electrospun polymer nanofibers: An overview. *Journal of Molecular Catalysis B: Enzymatic* **2009**, *56*, 189-195.
18. Al-Attabi, R.; Morsi, Y.; Schütz, J.A.; Dumée, L.F. One-pot synthesis of catalytic molybdenum based nanocomposite nano-fiber membranes for aerosol air remediation. *Science of The Total Environment* **2019**, *647*, 725-733.
19. Al-Attabi, R.; Dumée, L.F.; Schütz, J.A.; Morsi, Y. Pore engineering towards highly efficient electrospun nanofibrous membranes for aerosol particle removal. *Science of The Total Environment* **2018**, *625*, 706-715.
20. Vanangamudi A., Y.X., Duke M.C., Dumee L.F. . Nanofibers for membrane applications. . In *Handbook of nanofibers.*, In: Barhoum A., B.M., Makhlouf A. (eds) Ed. Springer, Cham: 2018.
21. Jia, H.; Zhu, G.; Vugrinovich, B.; Kataphinan, W.; Reneker, D.H.; Wang, P. Enzyme-carrying polymeric nanofibers prepared via electrospinning for use as unique biocatalysts. *Biotechnology Progress* **2002**, *18*, 1027-1032.
22. Kim, T.G.; Park, T.G. Surface functionalized electrospun biodegradable nanofibers for immobilization of bioactive molecules. *Biotechnology Progress* **2006**, *22*, 1108-1113.
23. Srbová, J.; Slováková, M.; Křípalová, Z.; Žárská, M.; Špačková, M.; Stránská, D.; Bílková, Z. Covalent biofunctionalization of chitosan nanofibers with trypsin for high enzyme stability. *Reactive and Functional Polymers* **2016**, *104*, 38-44.
24. R. Silva, T.; Rodrigues, D.; Rocha, J.M.s.; Gil, H.; Pinto, S.; Lopes da Silva, J.; Guiomar, A.J. *Immobilization of trypsin onto poly(ethylene terephthalate)/poly(lactic acid) nonwoven nanofiber mats*. 2015; Vol. 104.
25. Ray, S.S.; Chen, S.-S.; Li, C.-W.; Nguyen, N.C.; Nguyen, H.T. A comprehensive review: Electrospinning technique for fabrication and surface modification of membranes for water treatment application. *RSC Advances* **2016**, *6*, 85495-85514.
26. Schulze, A.; Breite, D.; Kim, Y.; Schmidt, M.; Thomas, I.; Went, M.; Fischer, K.; Prager, A. Bio-inspired polymer membrane surface cleaning. *Polymers* **2017**, *9*.
27. Schulze, A.; Stoelzer, A.; Striegler, K.; Starke, S.; Prager, A. Biocatalytic self-cleaning polymer membranes. *Polymers* **2015**, *7*.
28. Moreno-Cortez, I.E.; Romero-García, J.; González-González, V.; García-Gutierrez, D.I.; Garza-Navarro, M.A.; Cruz-Silva, R. Encapsulation and immobilization of papain in electrospun nanofibrous membranes of pva cross-linked with glutaraldehyde vapor. *Materials Science and Engineering: C* **2015**, *52*, 306-314.

549 29. Tripathi, B.P.; Dubey, N.; Simon, F.; Stamm, M. *Thermo responsive ultrafiltration membranes of*
550 *grafted poly(n-isopropyl acrylamide) via polydopamine*. 2014; Vol. 4.
551 30. Bae You, H.; Okano, T.; Kim Sung, W. Temperature dependence of swelling of crosslinked
552 poly(n,n′-alkyl substituted acrylamides) in water. *Journal of Polymer Science Part B: Polymer*
553 *Physics* **2003**, *28*, 923-936.
554 31. Xu, Y.; Shi, L.; Ma, R.; Zhang, W.; An, Y.; Zhu, X.X. Synthesis and micellization of thermo-
555 and ph-responsive block copolymer of poly(n-isopropylacrylamide)-block-poly(4-
556 vinylpyridine). *Polymer* **2007**, *48*, 1711-1717.
557 32. Zhou, Q.; Li 李建华, J.-h.; Yan, B.-f.; Wu 吴东, D.; Zhang 张其清, Q.-q. *Thermo-responsive and*
558 *antifouling pvdf nanocomposited membranes based on pnipaam modified tio2 nanoparticles*. 2014;
559 Vol. 32.
560 33. Guo, H.; Huang, J.; Wang, X. The alternate temperature-change cleaning behaviors of
561 pnipaam grafted porous polyethylene membrane fouled by proteins. *Desalination* **2008**, *234*,
562 42-50.
563 34. Zhou, S.; Xue, A.; Zhang, Y.; Li, M.; Wang, J.; Zhao, Y.; Xing, W. Fabrication of temperature-
564 responsive zro2 tubular membranes, grafted with poly (n-isopropylacrylamide) brush
565 chains, for protein removal and easy cleaning. *Journal of Membrane Science* **2014**, *450*, 351-361.
566 35. http://www.worthington-biochem.com/TRY/default.html.
567 36. Jia, F.; Narasimhan, B.; Mallapragada, S. Materials-based strategies for multi-enzyme
568 immobilization and co-localization: A review. *Biotechnology and Bioengineering* **2014**, *111*, 209-
569 222.
570 37. Yu, J.-Z.; Zhu, L.-P.; Zhu, B.-K.; Xu, Y.-Y. *Poly(n-isopropylacrylamide) grafted poly(vinylidene*
571 *fluoride) copolymers for temperature-sensitive membranes*. 2011; Vol. 366, p 176-183.
572 38. Kang, K.; Kan, C.; Yeung, A.; Liu, D. The immobilization of trypsin on soap-free p(mma-ea-
573 aa) latex particles. *Materials Science and Engineering: C* **2006**, *26*, 664-669.
574 39. Zhang, K.; Wu, S.; Tang, X.; Kaiser, N.K.; Bruce, J.E. A bifunctional monolithic column for
575 combined protein preconcentration and digestion for high throughput proteomics research.
576 *Journal of Chromatography B* **2007**, *849*, 223-230.
577 40. Shimomura, M.; Ohta, M.; Sugiyama, N.; Oshima, K.; Yamauchi, T.; Miyauchi, S. Properties
578 of [alpha]-chymotrypsin covalently immobilized on poly(acrylic acid)-grafted magnetite
579 particles. *Polym J* **1999**, *31*, 274-278.